



C–H and C–C bond activations of terminal alkynes in the presence of a heteronuclear Ru₃Au cluster

Micaela Hernández–Sandoval^a, Francisco J. Zuno–Cruz^a, María J. Rosales–Hoz^b, Marco A. Leyva^b, Noemi Andrade^a, Verónica Salazar^a, Gloria Sánchez–Cabrera^{a,*}

^aCentro de Investigaciones Químicas, Universidad Autónoma del Estado de Hidalgo, Ciudad Universitaria, Km 4.5 Carretera Pachuca–Tulancingo, Pachuca Hgo., 42184, Mexico

^bDepartamento de Química, Centro de Investigación y Estudios Avanzados del I. P. N., Apdo. postal 14-740, 07000 México D. F., Mexico

ARTICLE INFO

Article history:

Received 4 May 2011

Received in revised form

29 July 2011

Accepted 1 August 2011

Dedicated to Professor Kenneth G. Caulton, on the occasion of his 70th birthday, in recognition of his many contributions to the field of organometallic chemistry.

Keywords:

Heteronuclear clusters

Ruthenium

Gold

Alkynes

Acetylides

ABSTRACT

The reaction of compound [Ru₃(CO)₁₀(μ–Cl)(μ–AuPPh₃)] (**1**) with terminal alkynes HC≡CR; (R = C₆H₄–4–CH₃, C₆H₃–2,5–(CH₃)₂, C₆H₂–2,4,5–(CH₃)₃, C(CH₃) = CH₂, Si(CH₃)₃), under very mild conditions yielded isostructural compounds [Ru₃(CO)₉(μ–AuPPh₃)(μ₃–η²–⊥–C≡CR)] (R = C₆H₄–4–CH₃ (**2**), C₆H₃–2,5–(CH₃)₂ (**3**), C₆H₂–2,4,5–(CH₃)₃ (**4**), C(CH₃)=CH₂ (**5**), Si(CH₃)₃ (**6**)) respectively; where the alkynes suffer oxidative additions to the metallic fragment coordinating as acetylide groups in a μ₃–η²–perpendicular fashion by breaking the C_(sp)–H bond of the alkynes. The AuPPh₃ fragment remains without change in all compounds. All of these clusters have been characterized in solution by i.r. and n.m.r. spectroscopy and their structures have been established by single crystal X–ray diffraction studies.

© 2011 Elsevier B.V. All rights reserved.

1. Introduction

In the last three decades, the activation of C–H bonds of alkenes and alkynes promoted by transition-metal cluster complexes has been a major research theme in organometallic chemistry, as can be appreciated in the literature [1–7]. The alkyne–complexes obtained from these reactions have been considered as useful models for the chemisorption of small molecules on metal surfaces and as examples of reactions where carbon–carbon triple bond activation and reduction reactions occur [1]. Studies carried out so far involve both homo- and heteronuclear clusters [8,9], the potential advantage of this polynuclear compounds is related to the fact that several metal atoms linked together can provide specific sites of interaction between organic molecules and clusters [10]; besides the insertion of a different type of metal (heterometallic clusters) gives an inherit polarity to the heterometallic bond, which

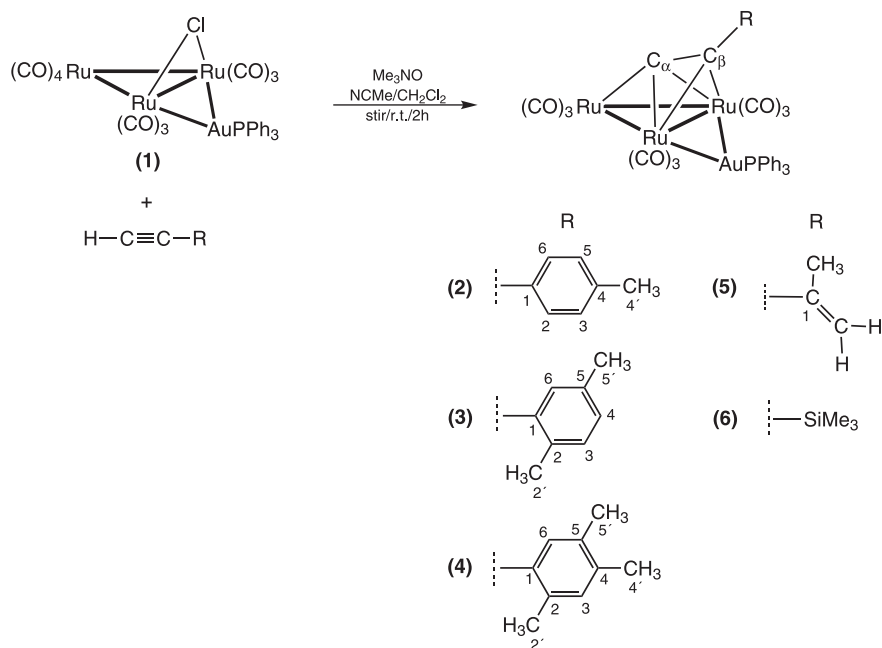
could direct and/or modify the substrate–catalyst interactions in catalytic processes for example in carbonylations [11], hydrogenations or HDS reactions of organic substrates [12].

To take advantage of this inherit polarity of the heterometallic bond in catalytic processes, the catalyst must be stable enough to produce the desire transformation in the substrate. It is well known that the carbonyl tetranuclear fragment Ru₃(AuPPh₃) lacks of kinetic stability since easily transforms by breaking its Ru–Au and Au–P bonds [13], avoiding its possible use as catalyst. Therefore the substitution of carbonyl ligands in this cluster by diphosphines or acetylides enhances the metallic core stability [14–16].

Thus, the potential application of alkyne clusters in catalysis leads to the study of these systems, for example the synthesis of homo- and heteronuclear transition metal carbonyl cluster involving different types of main group heteroatoms, bonded to the metal core, have shown unique catalytic properties [11,17–21]. Several mixed Ru–Au metal clusters containing hydride or carbon atoms [22–25], thiolates [26], diphosphines [27] and alkynes [28–31] among other ligands [32,33] have been reported elsewhere. Besides, a novel dynamic process operating in the [Fe₃(CO)₉(μ–AuPPh₃)(μ₃–η²–⊥–C≡CBu^t)] cluster has been

* Corresponding author. Tel.: +52 771 7172000x2204, +52 1771 1300735 (cell); fax: +52 771 7172000x6502.

E-mail address: gloriasa@uaeh.edu.mx (G. Sánchez–Cabrera).



Scheme 1. Synthesis of the acetylide ruthenium–gold clusters 2–6.

Table 1
¹H, ³¹P{¹H}, ²⁹Si{¹H} and ¹³C{¹H} NMR^a data for compounds 2–6.

Compound	¹ H δ(ppm) J(Hz)	³¹ P{ ¹ H} δ(ppm)	²⁹ Si{ ¹ H} δ(ppm) J(Hz)	¹³ C{ ¹ H} δ(ppm) J(Hz)	[C _α + C _β] {C _α –C _β }	
2	7.50 (m, 15H, Ph)	62.0 (s)	–	171.7 (s, C _α)	131.4 (d, C _β)	[271.9]
	7.44 (H _{AA'} , 2H, H(2,6))			138.0 (s, C(4))	⁴ J _{13C–31P} = 2.3	{71.5}
	7.13 (H _{BB'} , 2H, H(3,5))			134.1 (d, C _o)	131.1 (s, C(2, 6))	
	J _{AB} , J _{A'B'} = 7.9, J _{AA'} = 6.2, J _{BB'} = 1.8			² J _{13C–31P} = 14.6	129.5 (s, C(3, 5))	
	2.37 (s, 3H, CH ₃ (4'))			133.0 (s, C(1))	129.3 (d, C _m)	
				131.2 (d, C _i)	³ J _{13C–31P} = 10.8	
3	7.50 (m, 15H, Ph)	61.9 (s)	–	100.2 (s, C _β)	21.4 (s, CH ₃ (4'))	[268.5]
	7.21 (s, 1H, H(2))			172.2 (s, C _α)	131.2 (d, C _i)	{75.9}
	7.11 (d, 1H, H(5))			135.6 (s, C(1))	¹ J _{13C–31P} = 48.5	
	³ J _{H–1H} = 7.4			135.3 (s, C(3))	129.5 (s, C(4))	
	6.95 (d, 1H, H(4))			134.9 (s, C(6))	129.3 (d, C _m)	
	³ J _{H–1H} = 7.4			134.0 (d, C _o)	³ J _{13C–31P} = 11.2	
4	7.51 (m, 15H, Ph)	62.5 (s)	–	² J _{13C–31P} = 14.5	128.5 (s, C(5))	[268.3]
	7.17 (d, 1H, H(6))			133.3 (s, C(2))	96.3 (s, C _β)	{75.2}
	7.00 (d, 1H, H(3))			131.4 (d, C _o)	22.3 (s, CH ₃ (5'))	
	2.49 (s, 3H, CH ₃ (2'))			⁴ J _{13C–31P} = 2.1	21.0 (s, CH ₃ (2'))	
	2.25 (s, 3H, CH ₃ (4'))			171.7 (s, C _α)	131.3 (d, C _i)	
	2.20 (s, 3H, CH ₃ (5'))			136.5 (s, C(1))	¹ J _{13C–31P} = 48.4	
5	7.47 (m, 15H, Ph)	61.7 (s)	–	135.3 (s, C(5))	131.0 (d, C _i)	[275.6]
	5.26 (s, 1H, CH ₂ ^{cis})			134.3 (s, C(4))	¹ J _{13C–31P} = 48.3	{70.2}
	5.14 (m, 1H, CH ₂ ^{trans})			134.0 (d, C _o)	129.2 (d, C _m)	
	⁴ J _{H–1H} = 1.7			² J _{13C–31P} = 14.6	³ J _{13C–31P} = 10.8	
	2.15 (s, 3H, CH ₃)			131.3 (d, C _β)	117.9 (s, CH ₂)	
				⁴ J _{13C–31P} = 2.3	102.7 (s, C _β)	
6	7.47 (m, 15H, Ph)	62.3 (s)	0.8 (s)	26.7 (s, CH ₃)	131.0 (d, C _i)	[275.6]
	0.32 (s, 9H, CH ₃)			184.5 (s, C _α)	131.2 (d, C _i)	{101.5}
	² J _{H–29Si} = 6.6			134.0 (d, C _o)	¹ J _{13C–31P} = 48.4	
	² J _{H–29Si} = 13.2			² J _{13C–31P} = 14.6	129.2 (d, C _m)	
	¹ J _{H–13C} = 119.9			131.3 (d, C _β)	³ J _{13C–31P} = 10.8	
	¹ Δ ^{13/12} C = –1.1 ppb			⁴ J _{13C–31P} = 2.3	83.0 (s, C _β)	
		1.6 (s, 3C, CH ₃)				

^a Obtained at r. t. in CDCl₃, (s) singlet, (d) doublet, (m) multiplet, *o*, *ortho*; *p*, *para*; *m*, *meta*; *i*, *ipso*.

described, which involves the reversible rupture of a Au–Fe/Au–C_(acetylide) bonds [34]. Examples like this may produce useful information about bond cleavage that take place between the metallic fragment and organic substrate in catalytic reactions.

Despite all cluster reactions involving terminal alkynes that have been described [8,35]; there are some examples of Ru–Au tetranuclear complex with this type of ligands [36]. The methods to produce the desired Ru₃Au–Acetylide clusters mainly have been based on reactions between [Ru₃(CO)₁₂] or [Ru₃(CO)₁₀(NCMe)₂] and an Au–alkynyl ligand [15,16] or between the hydride acetylide ruthenium cluster and a suitable Au fragment as AuClPPh₃ [29] or [AuPPh₃]₃O⁺ [37]. Since the major previously reported synthetic method to prepare Ru₃Au acetylide complexes involves the preparation of a suitable gold–alkynyl precursor followed by a reaction with the Ru₃ homonuclear cluster [15,16,27,38,39], this prevents its wide use to produce this type of compounds. Therefore, in an effort to expand the available information on these systems, in this paper we report the synthesis and characterization of five new tetranuclear heterometallic ruthenium–gold clusters complexes containing acetylide ligands that arise from the cleavage of the C_(sp)–H bonds of terminal alkynes: [Ru₃(CO)₉(μ–AuPPh₃)(μ₃–η²–⊥–C≡CR)] (R = C₆H₄–4–CH₃ (**2**), C₆H₃–2,5–(CH₃)₂ (**3**), C₆H₂–2,4,5–(CH₃)₃ (**4**), C(CH₃)=CH₂ (**5**), Si(CH₃)₃ (**6**)). All compounds were prepared under mild conditions by the *in situ* reaction of compound [Ru₃(CO)₁₀(μ–Cl)(μ–AuPPh₃)] (**1**) and 1–ethynyl–2–methylbenzene, 1–ethynyl–2,5–dimethylbenzene, 1–ethynyl–2,4,5–trimethylbenzene, 2–methyl–1–buten–3–yne or trimethylsilylacetylene respectively. All synthesized compounds were characterized in solution by Infrared and ¹H, ¹³C{¹H}, ³¹P{¹H} and ²⁹Si{¹H} NMR spectroscopy. Full assignment of carbon atoms for all compounds was accomplished by 2–D heteronuclear correlation experiments. The molecular structures of all compounds in the solid state were determined by single crystal X–ray diffraction studies.

2. Results and discussion

Treatment of a CH₂Cl₂ solution of [Ru₃(CO)₁₀(μ–Cl)(μ–AuPPh₃)] (**1**), prepared *in situ* as previously described [26] with an excess of the appropriate terminal alkyne at room temperature (r. t.) for 2 h in the presence of Me₃NO as activating agent, leads to the formation of the new clusters [Ru₃(CO)₉(μ–AuPPh₃)(μ₃–η²–⊥–C≡CR)] (R = C₆H₄–4–CH₃ (**2**), C₆H₃–2,5–(CH₃)₂ (**3**), C₆H₂–2,4,5–(CH₃)₃ (**4**), C(CH₃)=CH₂ (**5**), Si(CH₃)₃ (**6**)) respectively in moderated yields (Scheme 1). In the case of methylated aryl series small amounts of isolobal compounds were observed, in which the AuPPh₃ fragment is replaced by a hydride ligand. In each reaction the main product is obviously derived from the C_(sp)–H bond cleavage in every alkyne and the substitution of the chlorine atom in the parent cluster. We employed different substituents: a series of variously methylated aryl derivatives, an olefinic fragment and a silicon group, to see if any steric or electronic inductive effect on the triple bond towards the reactivity of the heteronuclear cluster could be observed.

The symmetry of the i.r. spectra of all complexes is similar to those of the previously reported compounds [Ru₃(CO)₉(μ–AuPPh₃)(μ₃–η²–⊥–C≡CBu^t)] [29] and [Os₃(CO)₉(μ–AuPPh₃)(μ₃–η²–⊥–C≡CPh)] [30] (see experimental section). All compounds have isolobal structures to the well known trinuclear hydride acetylide complexes [Ru₃(CO)₉(μ–H)(μ₃–η²–⊥–C≡CR)] (R = Bu^t, SiMe₃, SiPh₃ [8], and C₆H₄–4–CH₃, C₆H₃–2,5–(CH₃)₂, C₆H₂–2,4,5–(CH₃)₃) (this work, see experimental section). There was no evidence of any influence of the substituent in the alkyne, that affects the CO stretch frequency, but the presence of a gold atom instead of the hydride ligand on the metallic skeleton indeed lowers the CO stretching frequencies.

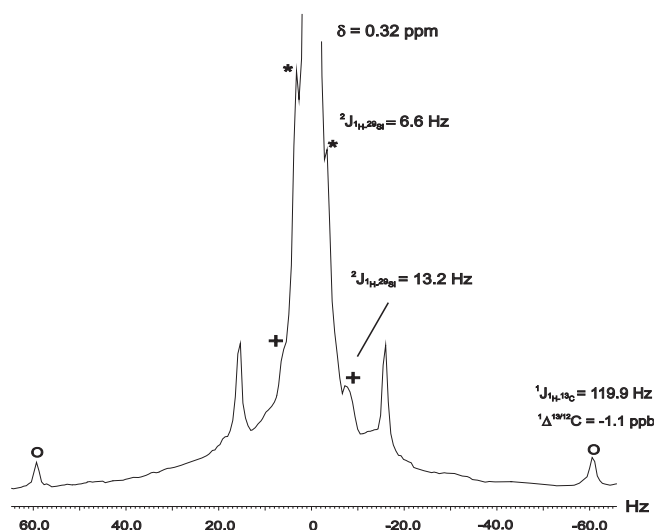


Fig. 1. ¹H NMR spectrum in the methyl region for compound **6**.

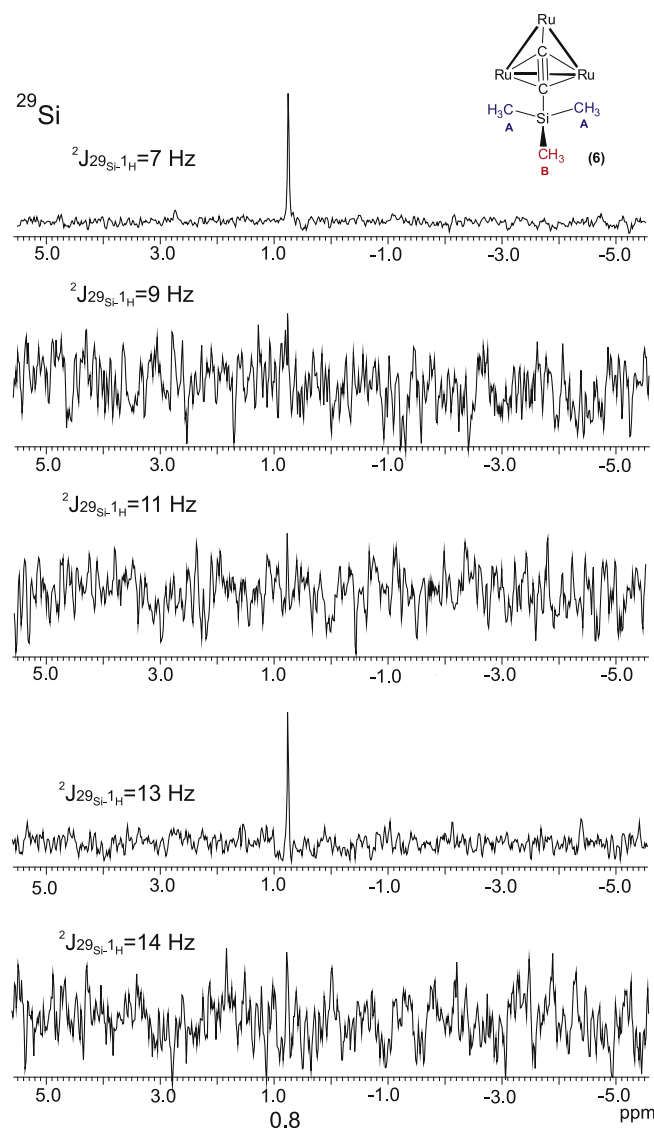


Fig. 2. ²⁹Si NMR spectra for **6**. CO and AuPPh₃ groups in the structure have been omitted for clarity.

(31.3 ppm). The fact that the compound **5** has the lowest polarization on the triple bond could be associated to a delocalized electronic effect due to the presence of the C=C bond substituent. This is supported by the charge alteration over the triple bond assumed to be evaluated by the $\delta(C_\alpha) + \delta(C_\beta)$ value, since compound **5** shows the largest value of all compounds. This fact could be related to an electronic inductive effect of the substituents.

2.1. X-ray diffraction studies

Single crystal X-ray diffraction studies were carried out to confirm the solid state structures of all synthesized compounds and to verify that there were no important structural differences in the described complexes. ORTEP diagrams of the structures are shown in Figs. 3 to 7 and Table 2 collects some selected bond lengths and angles. Compound **3** contains two crystallographically independent molecules in the asymmetric unit; both are essentially identical and only one of the two molecules is shown in Fig. 4. All compounds have a “butterfly” metal framework array with the gold atom occupying a wing-tip position. No significant differences in bond distances and angles in compounds **2** to **6** and related complexes $[\text{Ru}_3(\text{CO})_9(\mu\text{-AuPPh}_3)(\mu_3\text{-}\eta^2\text{-}\perp\text{-C}\equiv\text{C}\text{Bu}^t)]$ [29], $[\text{Ru}_3(\text{CO})_9(\mu\text{-AuPPh}_3)(\mu_3\text{-}\eta^2\text{-}\perp\text{-C}\equiv\text{C}\text{Fc})]$ [28] were observed. Similarly to compound $[\text{Ru}_3(\text{CO})_{10}(\mu\text{-AuPPh}_3)(\mu\text{-Cl})]$ [13] and some other ruthenium–gold clusters [24,28,29] the AuPPh₃ fragment is symmetrically coordinated bridging the largest Ru–Ru bond (Ru(1)–Ru(2) = 2.8415 Å av.).

It is also worth noticing that this average distance is smaller than those observed in other tetranuclear ruthenium–gold clusters containing a $\mu_3\text{-S}\text{Bu}^t$ (2.950(1) Å) [32] or $\mu_3\text{-PPh}$ (3.002(6) Å) [33] even though they have the same metal framework. Compounds **6** and **4** have larger Ru(1)–Ru(2) distances (2.8534(9) and 2.8507(11) Å respectively) than compounds **5**, **3** and **2**, [2.8331(6), 2.8416 av. and 2.8287(5) Å respectively]. Also, these bond distances are equal or slightly shorter than the “normal” Ru–Ru bond (2.854 Å av.) in $[\text{Ru}_3(\text{CO})_{12}]$, while in the cluster $[\text{Ru}_3(\text{CO})_{10}(\mu\text{-Cl})(\mu\text{-AuPPh}_3)]$ (1) the doubly bridged Ru–Ru bond (2.8742(6) Å) being the largest of all [13]. The other two Ru–Ru distances, Ru(2)–Ru(3) and Ru(3)–Ru(1) [2.8088 and 2.8070 Å av. respectively] are the shortest ones, which could be related to a higher polarization in the coordinated acetylide fragment as mentioned previously. The phosphine ligand is terminally attached to the gold atom with a P(1)–Au(1) average distance of 2.296 Å. All the C(1)–C(2) distances (range from 1.302(7) to 1.330(14) Å) in the acetylide fragments are closer to a C–C double bond distance ($C_{sp}\text{-}C_{sp}$ 1.21 Å; $C_{sp2}\text{-}C_{sp2}$ 1.34 Å; $C_{sp3}\text{-}C_{sp3}$ 1.53 Å [42]) reflecting the change in hybridization of these carbons upon coordination.

The Ru(3)–C(1)–C(2) angles are in the range of 153.3(4) – 155.6(8)°, while the C(1)–C(2)–C(3) angles for compounds **2**; 141.0(5)°, **3**; 145.5(5)° and 143.5(5)°, **4**; 144.4(4)° and **5**; 143.1(6)° and C(1)–C(2)–Si(1) for **6**; 144.0(8)°; both groups of angles are essentially the same than the corresponding values for $[\text{Ru}_3(\text{CO})_9(\mu\text{-AuPPh}_3)(\mu_3\text{-}\eta^2\text{-}\perp\text{-C}\equiv\text{C}\text{Bu}^t)]$ [29] and $[\text{Ru}_3(\text{CO})_9(\mu\text{-H})]$

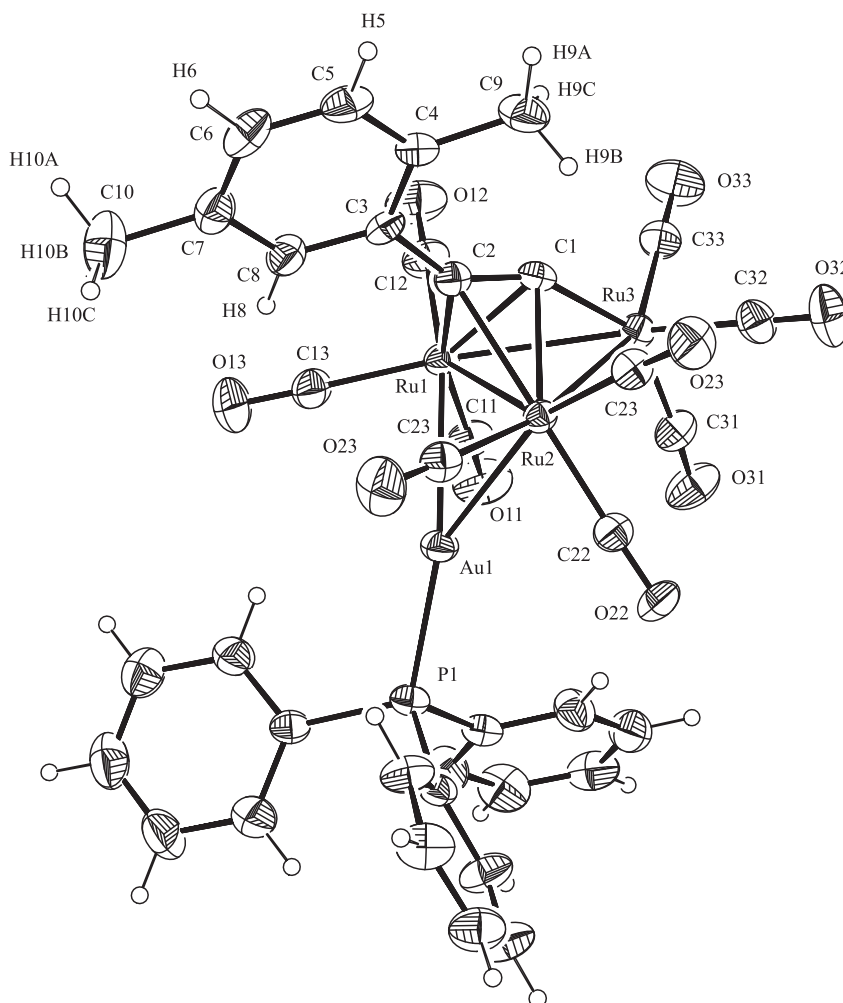


Fig. 4. ORTEP view of compound **3** (30% probability).

($\mu_3-\eta^2-\perp-C\equiv CR$) [8]. The trend observed in C(1)–C(2)–R angles among compounds $3_{(1)} \cong 4 \cong 6 > 5 > 2$ could be associated with a decrease in size of the substituent. The dihedral angles formed by the two planes [Ru(3)–Ru(1)–Ru(2) and Ru(1)–Ru(2)–Au(1)] for the heteronuclear butterfly core, are in the range of 110.30(2) to 121.28(1)°, with the SiMe₃ substituted acetylide showing the lowest value; this is probably due to its inherent hindrance properties. On the other hand, the type of substituents on C(2) (C_β), does not affect the interline angle between C(1)–C(2) and Ru(1)–Ru(2) with an average of 89.1°. No significant intermolecular short contacts were found in any crystal packing of collected compounds.

3. Conclusions

The study of tetraheteronuclear ruthenium–gold clusters of general formula [Ru₃(CO)₉(μ–AuPPh₃)(μ₃–η²–⊥–C≡CR)] shows that change in the substituents on the terminal alkynes does not significantly affect either the spectroscopic data or the main skeletal fragments of these clusters in the solid state. However, the ¹³C NMR data shows that there is some degree of polarization of the acetylide C–C bond being the lowest in compound **5**, which could be associated to a delocalized electronic effect due to the unsaturated substituent.

The synthesis of this type of compounds is a clear example of the ease of activation of C_(sp)–H and C_(sp)–C_(sp) bonds in alkynes promoted by a heterometallic ruthenium–gold cluster, through the rupture of the C–H bond and the re–hybridization of the acetylenic carbon atoms, establishing a simple synthetic route to this well–known class of compounds.

On the other hand, the well known thermodynamically stability of the Ru₃(AuPPh₃)(C₂R) fragment was confirmed since no decomposition in solution or in the solid state were observed for all compounds; this can be exploited, as mentioned before, in future potential catalytic applications as hydrogenation or HDS processes.

4. Experimental section

4.1. General procedures and materials

All reactions were carried out under nitrogen atmosphere. Solvents were dried prior to use by standard techniques and trimethylamine *N*–oxide dihydrate was sublimed several times in high–vacuum to remove water. All chemicals were supplied by Aldrich Company except chloro(triphenylphosphine)gold(I) which was supplied by Strem Chemicals, all reagents were used without further purifications. Commercial TLC plates (silica gel 60 F254) were used to monitor the progress of the reactions. Infrared spectra for all compounds were recorded in KBr pellets on a GX PERKIN Elmer 2000 FT–IR instrument. NMR spectra were measured on a JEOL Eclipse 400, JEOL GSX–270 and VARIAN 400 spectrometers in CDCl₃, with ¹H, ¹³C and ²⁹Si spectra relative to SiMe₄, and ³¹P spectra relative to 85% aq. H₃PO₄. Mass spectra were recorded at CINVESTAV–México (HR–LC 1100/MSD TOF Agilent Technology equipment). Compound **1** was prepared accordingly to published procedure [26].

4.2. General procedure for the synthesis of compounds

[Ru₃(CO)₉(μ–AuPPh₃)(μ₃–η²–⊥–C≡CR)] (R = C₆H₄–4–CH₃ (**2**), C₆H₃–2,5–(CH₃)₂ (**3**), C₆H₂–2,4,5–(CH₃)₃ (**4**), C(CH₃)=CH₂ (**5**), Si(CH₃)₃ (**6**))

To the solution of [Ru₃(CO)₁₀(μ–Cl)(μ–AuPPh₃)] (**1**) was added “*in situ*” an excess of the corresponding alkyne and 1.5 equivalent amount of dry Trimethylamine *N*–oxide, (CH₃)₃NO. Every reaction mixture was stirred for 2 h. The solvent was removed under low pressure and the resulting residue was redissolved in a minimum

amount of chloroform and separated by TLC (eluent: hexane–chloroform (80:20 v/v).

4.3. [Ru₃(CO)₉(μ–AuPPh₃)(μ₃–η²–⊥–C≡CR)] (R = C₆H₄–4–CH₃) (**2**)

The above procedure was employed for the preparation of **2**. The following compounds were used: [Ru₃(CO)₁₀(μ–Cl)(μ–AuPPh₃)] (**1**) (50.0 mg, 0.050 mmol), 1–etynyl–2–methylbenzene (16 mg; 0.111 mmol) and (CH₃)₃NO, (6 mg, 0.080 mmol). The first band was identified as traces of starting material, the second band was identified as compound [Ru₃(CO)₉(μ–H)(μ₃–η²–⊥–C≡CC₆H₄–4–CH₃)] Yield: (yellow solid, 4 mg, 12%). ¹H NMR in CDCl₃ at 298 K: 7.46 (d, 2H, H(2,6), ³J = 7.5 Hz), 7.16 (d, 2H, H(3,5), ³J = 7.5 Hz), 2.38 (s, 3H, CH₃(4')), –20.51 (s, 1H, Ru–H–Ru). IR ν(CO): 2097(w), 2073(m), 2053(m), 2022(vs), 1986(w) cm^{–1}. The sixth band corresponds to compound [Ru₃(CO)₉(μ–AuPPh₃)(μ₃–η²–⊥–C≡CC₆H₄–4–CH₃)] (**2**). Yield: (yellow solid, 16 mg, 32%). HR–MS (ESI–TOF); [MH]⁺ for (C₃₆H₂₃O₉PRu₃Au) calcd 1132.7870, found +1132.7862. IR ν(CO): 2072 (m), 2053 (sh), 2033 (vs), 2004 (s), 1991 (sh), 1985 (s), 1959 (s), 1943 (sh) cm^{–1}. The remaining bands were not studied because they did not contain coordinated ligands accordingly to their ¹H NMR spectrums.

4.4. [Ru₃(CO)₉(μ–AuPPh₃)(μ₃–η²–⊥–C≡CR)] (R = C₆H₃–2,5–(CH₃)₂) (**3**)

The general procedure was employed for the preparation of **3**. The following compounds were used: [Ru₃(CO)₁₀(μ–Cl)(μ–AuPPh₃)] (**1**) (50.0 mg, 0.050 mmol), 1–etynyl–2,5–dimethylbenzene (18 μl;

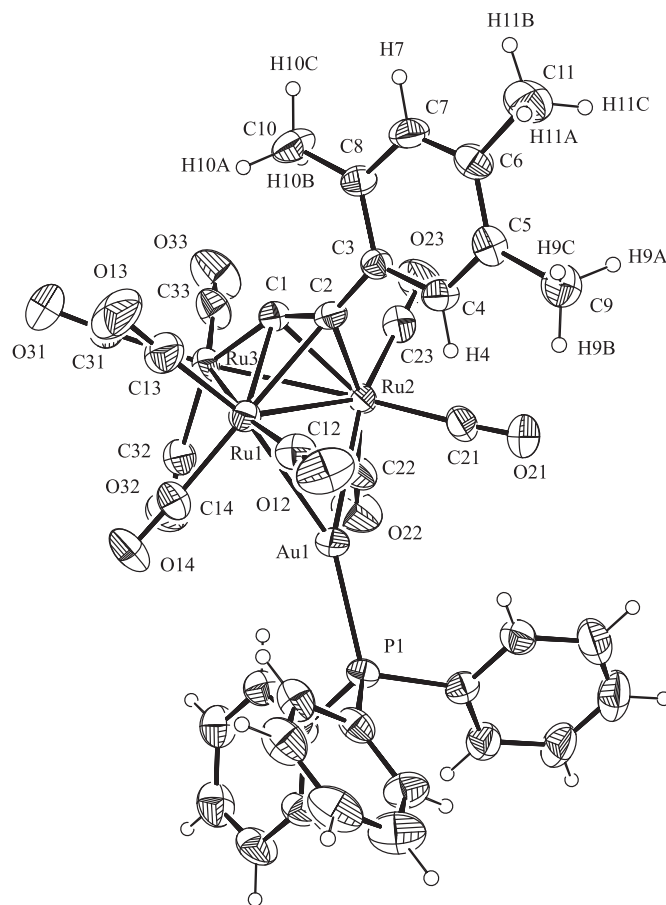


Fig. 5. ORTEP view of compound **4** (30% probability).

0.130 mmol) and $(\text{CH}_3)_3\text{NO}$, (6 mg, 0.080 mmol). The first band was identified as traces of starting material, the second band was identified as compound $[\text{Ru}_3(\text{CO})_9(\mu\text{-H})(\mu_3\text{-}\eta^2\text{-}\perp\text{-C}\equiv\text{CC}_6\text{H}_4\text{-2,5-(CH}_3)_2)]$ (3). Yield: (yellow solid, 11 mg, 22%). HR-MS (ESI-TOF); $[\text{MH}]^+$ for $(\text{C}_{37}\text{H}_{25}\text{O}_9\text{PRu}_3\text{Au})$ calcd 1146.8026, found +1146.8028. IR $\nu(\text{CO})$: 2071(m), 2052(sh), 2030(vs), 1990(s, br), 1968(sh), 1959(sh) cm^{-1} . The fifth band corresponds to compound $[\text{Ru}_3(\text{CO})_9(\mu\text{-AuPPh}_3)(\mu_3\text{-}\eta^2\text{-}\perp\text{-C}\equiv\text{CC}_6\text{H}_4\text{-2,5-(CH}_3)_2)]$ (4). Yield: (yellow solid, 15 mg, 30%). HR-MS (ESI-TOF); $[\text{MH}]^+$ for $(\text{C}_{38}\text{H}_{27}\text{O}_9\text{PRu}_3\text{Au})$ calcd 1160.8183, found +1160.8191. IR $\nu(\text{CO})$: 2069(m), 2038(sh), 2027(vs), 1998(s), 1987(s), 1978(s), 1967(m), 1961(m) cm^{-1} . The remaining bands were not studied because they did not contain coordinated ligands accordingly to their ^1H NMR spectra.

4.5. $[\text{Ru}_3(\text{CO})_9(\mu\text{-AuPPh}_3)(\mu_3\text{-}\eta^2\text{-}\perp\text{-C}\equiv\text{CR})]$
($R = \text{C}_6\text{H}_2\text{-2,4,5-(CH}_3)_3$) (4)

The general procedure was employed for the preparation of 4. The following compounds were used: $[\text{Ru}_3(\text{CO})_{10}(\mu\text{-Cl})(\mu\text{-AuPPh}_3)]$ (1) (50.0 mg, 0.050 mmol), 1-etynyl-2,4,5-trimethylbenzene (35 μl ; 0.276 mmol) and $(\text{CH}_3)_3\text{NO}$, (6 mg, 0.080 mmol). The first band was identified as traces of starting material, the second band was identified as compound $[\text{Ru}_3(\text{CO})_9(\mu\text{-H})(\mu_3\text{-}\eta^2\text{-}\perp\text{-C}\equiv\text{CC}_6\text{H}_4\text{-2,4,5-(CH}_3)_3)]$ (3). Yield: (yellow solid, 4.5 mg, 13%). ^1H NMR in CDCl_3 at 298 K: 7.19 (s, 1H, H(6)), 7.03 (s, 1H, H(3)), 3.73 (s, 3H, $\text{CH}_3(2')$), 2.48 (s, 3H, $\text{CH}_3(4')$), 2.26 (s, 3H, $\text{CH}_3(5')$), -20.37 (s, 1H, Ru-H-Ru). IR $\nu(\text{CO})$: 2096(m), 2068(vs), 2049(vs), 2013(vs), 1983(s) cm^{-1} . The fifth

band corresponds to compound $[\text{Ru}_3(\text{CO})_9(\mu\text{-AuPPh}_3)(\mu_3\text{-}\eta^2\text{-}\perp\text{-C}\equiv\text{CC}_6\text{H}_2\text{-2,4,5-(CH}_3)_3)]$ (4). Yield: (yellow solid, 15 mg, 30%). HR-MS (ESI-TOF); $[\text{MH}]^+$ for $(\text{C}_{38}\text{H}_{27}\text{O}_9\text{PRu}_3\text{Au})$ calcd 1160.8183, found +1160.8191. IR $\nu(\text{CO})$: 2069(m), 2038(sh), 2027(vs), 1998(s), 1987(s), 1978(s), 1967(m), 1961(m) cm^{-1} . The remaining bands were not studied because they did not contain coordinated ligands accordingly to their ^1H NMR spectra.

4.6. $[\text{Ru}_3(\text{CO})_9(\mu\text{-AuPPh}_3)(\mu_3\text{-}\eta^2\text{-}\perp\text{-C}\equiv\text{CR})]$ ($R = \text{C}(\text{CH}_3)=\text{CH}_2$) (5)

The general procedure was employed for the preparation of 5. The following compounds were used: $[\text{Ru}_3(\text{CO})_{10}(\mu\text{-Cl})(\mu\text{-AuPPh}_3)]$ (1) (50.0 mg, 0.050 mmol), 2-methyl-1-buten-3-yne (28 μl ; 0.300 mmol) and $(\text{CH}_3)_3\text{NO}$, (6 mg, 0.080 mmol). The first band was identified as traces of starting material and the second band corresponds to compound $[\text{Ru}_3(\text{CO})_9(\mu\text{-AuPPh}_3)(\mu_3\text{-}\eta^2\text{-}\perp\text{-C}\equiv\text{CC}(\text{CH}_3)=\text{CH}_2)]$ (5). Yield: (yellow solid, 11 mg, 22%). HR-MS (ESI-TOF); $[\text{MH}]^+$ for $(\text{C}_{32}\text{H}_{21}\text{O}_9\text{PRu}_3\text{Au})$ calcd 1082.7713, found +1082.7735. IR $\nu(\text{CO})$: 2093(m), 2069(s), 2049(sh), 2033(vs), 1990(vs, br), 1969(m), 1963(m), 1958(m) cm^{-1} .

4.7. $[\text{Ru}_3(\text{CO})_9(\mu\text{-AuPPh}_3)(\mu_3\text{-}\eta^2\text{-}\perp\text{-C}\equiv\text{CR})]$ ($R = \text{Si}(\text{CH}_3)_3$) (6)

The general procedure was employed for the preparation of 6. The following compounds were used: $[\text{Ru}_3(\text{CO})_{10}(\mu\text{-Cl})(\mu\text{-AuPPh}_3)]$ (1) (50.0 mg, 0.050 mmol), trimethylsilylacetylene (42 μl ; 0.300 mmol) and $(\text{CH}_3)_3\text{NO}$, (6 mg, 0.080 mmol). The first band was identified as traces of starting material and the second

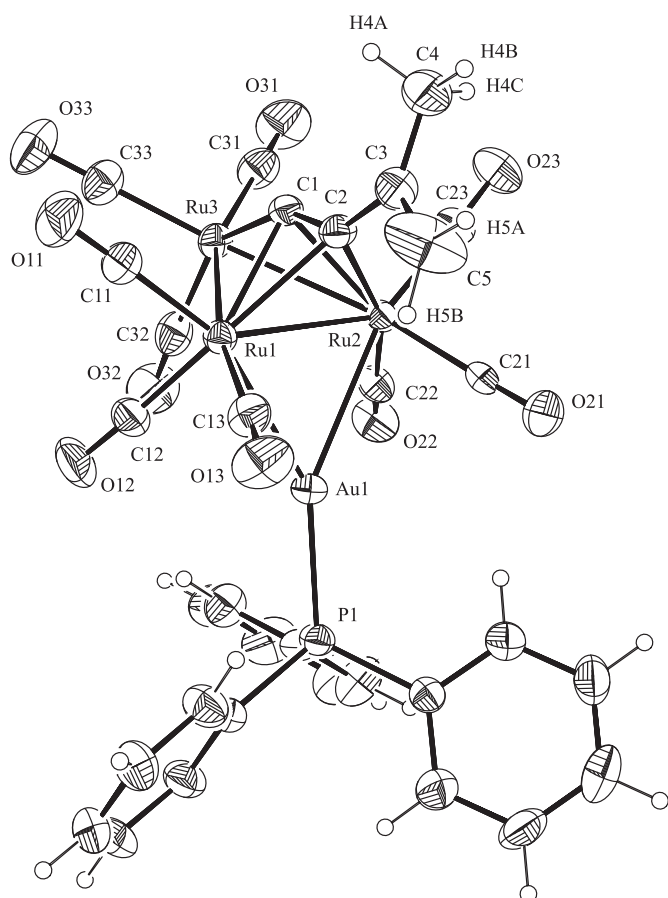


Fig. 6. ORTEP view of compound 5 (30% probability).

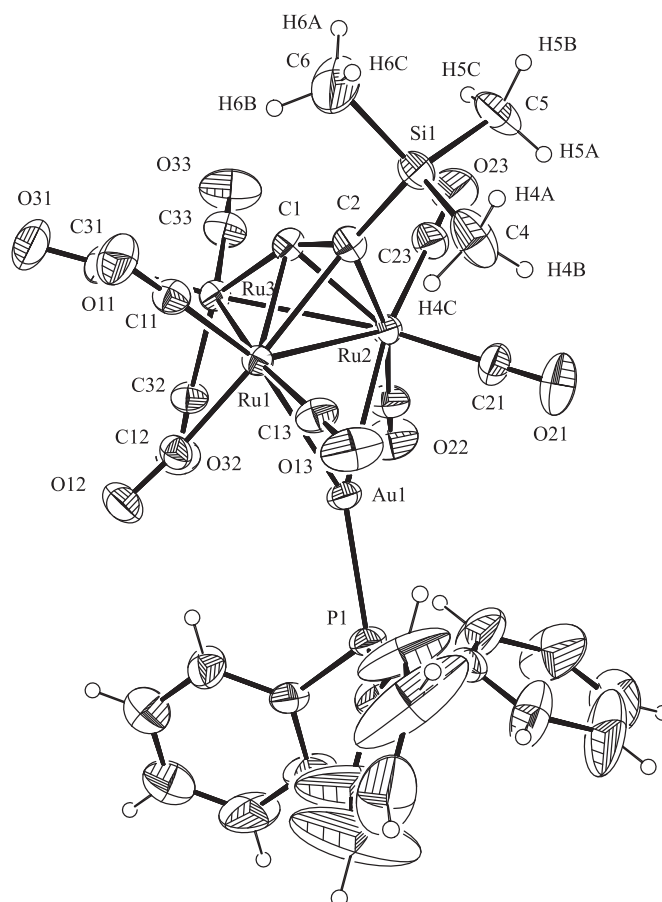


Fig. 7. ORTEP view of compound 6 (30% probability).

Table 2
Selected bond lengths (Å) and angles (°) for compounds 2–6.

Compound	2	3	4	5	6	
Bond lengths		Molecule1	Molecule2			
Ru(1)–Ru(2)	2.8287(5)	2.8448(6)	2.8383(6)	2.8507(11)	2.8331(6)	2.8534(9)
Ru(2)–Ru(3)	2.8103(5)	2.8138(6)	2.8036(7)	2.8167(12)	2.8023(7)	2.8063(10)
Ru(3)–Ru(1)	2.8269(6)	2.8088(6)	2.7869(6)	2.7996(12)	2.8100(7)	2.8099(9)
C(1)–C(2)	1.302(7)	1.314(7)	1.313(6)	1.330(14)	1.303(8)	1.330(13)
C(2)–Si(1)	–	–	–	–	–	1.855(10)
C(2)–C(3)	1.473(6)	1.461(7)	1.469(7)	1.444(13)	1.465(8)	–
Ru(1)–C(1)	2.185(5)	2.220(5)	2.197(5)	2.173(10)	2.202(6)	2.190(9)
Ru(1)–C(2)	2.231(4)	2.246(5)	2.244(5)	2.264(10)	2.237(6)	2.260(9)
Ru(2)–C(1)	2.190(5)	2.194(5)	2.182(5)	2.188(10)	2.192(6)	2.169(9)
Ru(2)–C(2)	2.254(4)	2.277(5)	2.241(5)	2.249(10)	2.247(6)	2.258(10)
Ru(3)–C(1)	1.947(5)	1.960(6)	1.941(5)	1.937(10)	1.950(6)	1.938(9)
Ru(1)–Au(1)	2.7652(4)	2.7734(5)	2.7739(5)	2.7487(9)	2.7597(5)	2.7659(7)
Ru(2)–Au81	2.7645(4)	2.7505(5)	2.7684(5)	2.7712(9)	2.7616(5)	2.7590(7)
Au(1)–P(1)	2.293(1)	2.295(2)	2.296(2)	2.296(2)	2.291(2)	2.306(2)
Bond angles						
Ru(1)–Ru(2)–Ru(3)	60.172(13)	59.518(15)	59.200(16)	59.20(3)	59.817(17)	59.53(2)
Ru(2)–Ru(3)–Ru(1)	60.237(14)	60.791(15)	61.021(16)	61.00(3)	60.637(16)	61.07(2)
Ru(3)–Ru(1)–Ru(2)	59.592(12)	59.691(15)	59.779(16)	59.79(3)	59.546(16)	59.40(2)
Ru(3)–C(1)–C(2)	154.9(4)	153.3(4)	153.5(4)	155.4(8)	153.4(4)	155.6(8)
C(1)–C(2)–C(3)	141.0(5)	145.5(5)	143.5(5)	144.4(9)	143.1(6)	–
C(1)–C(2)–Si(1)	–	–	–	–	–	144.0(8)
C(2)–Ru(1)–Au(1)	104.44(12)	101.11(14)	101.26(13)	101.5(2)	102.89(15)	104.6(3)
C(2)–Ru(2)–Au(1)	103.82(12)	100.96(13)	101.50(13)	101.3(3)	102.56(15)	104.8(2)
C(1)–Ru(1)–Au(1)	108.00(11)	107.92(13)	108.17(13)	108.3(3)	108.28(15)	105.9(2)
C(1)–Ru(2)–Au(1)	107.87(12)	109.50(13)	108.81(14)	107.1(3)	108.52(15)	106.8(2)
Interline and interplane angles						
C(1)–C(2)/Ru(1)–Ru(2)	89.5(2)	88.0(2)	89.6(3)	89.0(4)	89.3(3)	89.4(5)
C(1)–C(2)/Ru(3)–Ru(2)–Ru(1)	17.8(2)	17.2(3)	16.9(3)	17.5(4)	16.9(4)	18.4(5)
Ru(3)–Ru(1)–Ru(2)/Ru(1)–Ru(2)–Au(1)	114.32(1)	121.28(1)	119.83(1)	119.10(2)	117.15(2)	110.30(2)
C(1)–Ru(1)–Ru(2)/Ru(1)–Ru(2)–Au(1)	167.0(2)	174.6(2)	173.04(2)	172.0(3)	170.3(1)	163.1(3)
C(2)–Ru(1)–Ru(2)/Ru(1)–Ru(2)–Au(1)	148.2(1)	140.6(1)	141.6(1)	142.2(2)	144.9(2)	150.9(2)

Table 3
Crystal data and structure refinement parameters for compounds 2–6.

Compound	2	3	4	5	6
Empirical formula	C ₃₆ H ₂₂ Au ₁ O ₉ P ₁ Ru ₃	C ₃₇ H ₂₄ Au O ₉ P ₁ Ru ₃	C ₃₈ H ₂₆ Au ₁ O ₉ P ₁ Ru ₃	C ₃₂ H ₂₀ Au ₁ O ₉ P ₁ Ru ₃	C ₃₂ H ₂₄ Au ₁ O ₉ P ₁ Ru ₃ Si1
Formula weight	1129.68	1143.71	1157.73	1079.63	1111.75
Crystal colour and shape	red prism	orange prism	red prism	orange plate	orange prism
Crystal system	Monoclinic	Monoclinic	Monoclinic	Monoclinic	Monoclinic
Crystal size (mm)	0.3 × 0.2 × 0.1	0.28 × 0.11 × 0.1	0.25 × 0.21 × 0.15	0.41 × 0.39 × 0.21	0.25 × 0.19 × 0.091
Space group	P2 ₁ /c	P2 ₁ /n	C2/c	P2 ₁ /n	P2 ₁
Unit cell dimensions					
a (Å)	13.0243(2)	12.7175(3)	35.8213(11)	13.2217(2)	12.3295(2)
b (Å)	11.5864(2)	33.9779(8)	13.1804(5)	17.0832(3)	10.1494(2)
c (Å)	24.4145(4)	17.8827(4)	16.8224(5)	16.0699(3)	15.1613(3)
α (°)	90.00	90	90.00	90.00	90
β (°)	96.3720(10)	100.1460(10)	94.379(2)	107.9270(10)	102.2140(10)
γ (°)	90.00	90	90.00	90.00	90
V, (Å ³)	3661.50(10)	7606.5(3)	7919.3(5)	3453.47(10)	1854.29(6)
Z	4	8	8	4	2
D _{calcd} , (Mg m ⁻³)	2.049	1.997	1.942	2.076	1.991
μ, (mm ⁻¹)	5.304	5.108	4.907	5.618	5.265
Temperature (K)	293(2)	293(2)	293(2)	293(2)	293(2)
λ (Mo-Kα) (Å)	0.71073	0.71073	0.71073	0.71073	0.71073
Scan type	ω-φ	ω-φ	ω-φ	ω-φ	ω-φ
2θ range (°)	3.07 to 27.47	2.93 to 27.43	3.54 to 27.49	3.45 to 27.48	3.4 to 27.48
Index ranges					
(hmin/hmax, kmin/kmax, lmin/lmax)	-16/13, 13/15, -26/31	-16/13, 44/42, -22/23	-31/45, -15/17, -21/18	-17/16, -22/21, -20/20	-15/15, -13/11, -19/19
Reflections collected	22 163	41 476	18 593	37022	26051
Independent reflections	8112 (R _{int} = 0.0383)	16 544 (R _{int} = 0.0479)	8232 (R _{int} = 0.0635)	7878 (R _{int} = 0.0393)	4430 (R _{int} = 0.0393)
Observed reflections	5855 (F > 4σ(F))	4352 (F > 4σ(F))	5558 (F > 4σ(F))	5695 (F > 4σ(F))	4021 (F > 4σ(F))
Parameters/restraints	452/0	923/0	436/0	416/1	391/1
R _{final} ; R _{all} data	0.0383, 0.0676	0.0412, 0.0643	0.0635, 0.1045	0.0393, 0.0681	0.0338, 0.0403
Rw _{final} , R _w all data	0.0761, 0.0881 ^a	0.0855, 0.0744 ^b	0.1547, 0.1860 ^c	0.0793, 0.0681 ^d	0.0792, 0.0824 ^e
GOF (all data)	0.97	1.014	0.909	0.909	0.996
Max, min peaks (eÅ ⁻³)	0.937/-0.826	0.580/-0.746	0.782/-1.067	0.888/-1.148	0.781/-1.292

^a $w^{-1} = \sigma^2(F_o^2) + (0.0400P)^2 + P$.

^b $w^{-1} = \sigma^2(F_o^2) + (0.10.0062P)^2 + 5.5156P$.

^c $w^{-1} = \sigma^2(F_o^2) + (0.1131P)^2 + 51.5217P$.

^d $w^{-1} = \sigma^2(F_o^2) + (0.0322P)^2 + 4.6502P$.

^e $w^{-1} = \sigma^2(F_o^2) + (0.0485P)^2 + 1.2819P$. Where $P = (F_o^2 + 2F_c^2)/3$.

band corresponds to compound $[\text{Ru}_3(\text{CO})_9(\mu\text{-AuPPh}_3)(\mu_3\text{-}\eta^2\text{-}\perp\text{-C}\equiv\text{CSi}(\text{CH}_3)_3)]$ (**6**). Yield: (yellow solid, 13 mg, 25%). HR–MS (ESI–TOF); $[\text{MH}]^+$ for $(\text{C}_{32}\text{H}_{25}\text{O}_9\text{PSiRu}_3\text{Au})$ calcd 1114.7796, found +1114.7796. IR $\nu(\text{CO})$: 2070 (m), 2040 (sh), 2029 (vs), 2004 (s), 1994 (sh), 1980 (s), 1971 (sh), 1960 (m), 1946 (m) cm^{-1} .

5. Crystallography

Suitable crystals for compounds **2** to **6** were obtained by slow evaporation of CHCl_3 solution at low temperature (5°C) for several days. Table 3 shows details for data collection and structure refinement for all compounds. Data were collected in an Enraf–Nonius Cappa CCD area detector diffractometer using $\text{MoK}\alpha$ radiation. The samples were mounted in MicroMounts (MiTeGen company) www.mitegen.com. For all compounds, all non–hydrogen atoms were refined anisotropically. Hydrogen atoms were fixed at idealized refined positions. Data collection, determination of unit cell and integration of frames of all compounds were carried out using the suite Collect software [43] and HKL Scalepack [44]. A semi–empirical absorption correction method (SADABS) [45] was applied in all cases. All structures were resolved by direct methods, completed by subsequent difference Fourier synthesis, and refined by full–matrix least–squares procedures using the SHELX–97 package [45]. All crystallographic programs were used under WINGX program [46].

Acknowledgements

We gratefully acknowledge funding from Consejo Nacional de Ciencia y Tecnología CONACYT, Mexico, (Grants No.: J110.362/2007, CB–106849, 84453 and 025424) and PROM–EP–UAHGO–PTC–265. MHS thanks CONACYT for her scholarship.

Appendix A. Supplementary data

CCDC 821994, 830621, 821993, 821996 and 821995 contain the supplementary crystallographic data for **2** to **6** respectively. These data can be obtained free of charge from The Cambridge Crystallographic Data Centre via www.ccdc.cam.ac.uk/data_request/cif.

References

- [1] E. Sappa, A. Tiripichio, P. Braunstein, *Chem. Rev.* **83** (1983) 203–239.
- [2] P.R. Raithby, M.J. Rosales, *Adv. Inorg. Chem. Radiochem* **29** (1985) 169–247 (and references therein).
- [3] M.I. Bruce, in: G. Wilkinson, F. Gordon, A. Stone, E.W. Abel (Eds.), *Comprehensive Organometallic Chemistry I*, vol. 4, Pergamon Press., Oxford, 1982, pp. 843–887 (and references therein).
- [4] J.A. Cabeza, E. Pérez–Carreño, *Organometallics* **27** (2008) 4697–4702.
- [5] Y.L.K. Tan, W.K. Leong, *J. Organomet. Chem.* **692** (2007) 768–773.
- [6] W.-Y. Yeh, K.-Y. Tsai, *Organometallics* **29** (2010) 604–609.
- [7] P.R. Raithby, A.L. Johnson, in: R. Crabtree, M. Mingos (Eds.), *Comprehensive Organometallic Chemistry III*, vol. 6, Elsevier Science, 2006, pp. 766–773 (and references therein).
- [8] F.J. Zuno–Cruz, A.L. Carrasco, M.J. Rosales–Hoz, *Polyhedron* **21** (2002) 1105–1115.
- [9] I.D. Salter, in: P. Braunstein, L.A. Oro, P.R. Raithby (Eds.), *Metal Clusters in Chemistry*, vol. I, Wiley–VCH, Germany, 1999, pp. 509–534 (and references therein).
- [10] J.A. Cabeza, in: P. Braunstein, L.A. Oro, P.R. Raithby (Eds.), *Metal Clusters in Chemistry*, vol. II, Wiley–VCH, Germany, 1999, pp. 715–740 (and references therein).
- [11] Y. Li, W.–T Wong, *Eur. J. Inorg. Chem.* (2003) 2651–2662.
- [12] P. Braunstein, J. Rosé, in: P. Braunstein, L.A. Oro, P.R. Raithby (Eds.), *Metal Clusters in Chemistry*, vol. II, Wiley–VCH, Germany, 1999, pp. 617–677 (and references therein).
- [13] G. Lavigne, F. Papageorgiou, J.–J Bonnet, *Inorg. Chem.* **23** (1984) 609–613.
- [14] M.I. Bruce, M. Gaudio, B.W. Skelton, A. Werth, A.H. White, *Z. Anorg. Allg. Chem.* **634** (2008) 1106–1110.
- [15] M.I. Bruce, M. Gaudio, G. Melino, N.N. Zaitseva, B.K. Nicholson, B.W. Skelton, A.H. White, *J. Cluster Sci* **19** (2008) 147–170.
- [16] W.M. Khairul, L. Porres, D. Albesa–Jove, M.S. Senn, M. Jones, D.P. Lydon, J.A.K. Howard, A. Beeby, T.B. Marder, P.J. Low, *J. Cluster Sci.* **17** (2006) 65–85.
- [17] R.D. Adams, E. Trufan, *Phil. Trans. Royal Soc.* **368** (2010) 1473–1493.
- [18] R.D. Adams, B. Captain, *Angew. Chem. Int. Ed.* **47** (2008) 252–257.
- [19] J. Evans, G. Jingxing, *J. Chem. Soc. Chem. Commun.* (1985) 39–40.
- [20] P. Homanen, R. Persson, M. Haukka, T.A. Pakkanen, E. Nordlander, *Organometallics* **19** (2000) 5568–5574.
- [21] P. Frediani, A. Salvini, S. Finocchiaro, *J. Organomet. Chem.* **584** (1999) 265–273.
- [22] M.I. Bruce, P.A. Humphrey, B.W. Skelton, A.H. White, *J. Organomet. Chem.* **689** (2004) 2558–2561.
- [23] M.I. Bruce, P.A. Humphrey, B.W. Skelton, A.H. White, *J. Organomet. Chem.* (1997) 545–546 pp. 207–218.
- [24] M. Green, K.A. Mead, R.M. Mills, I.D. Salter, F. Gordon, A. Stone, P. Woodward, *J. Chem. Soc. Chem. Commun.* (1982) 51–53.
- [25] L.W. Bateman, M. Green, J.A.K. Howard, K.A. Mead, R.M. Mills, I.D. Salter, F. Gordon, A. Stone, P. Woodward, *J. Chem. Soc. Chem. Commun.* (1982) 773–775.
- [26] M.G. Hernández–Cruz, G. Sánchez–Cabrera, M. Hernández–Sandoval, M.A. Leyva, M.J. Rosales–Hoz, B.A. Ordoñez–Flores, V. Salazar, A. Guevara Lara, F.J. Zuno–Cruz, *J. Organomet. Chem.* **696** (2011) 2177–2185.
- [27] W.M. Khairul, D. Albesa–Jove, D.S. Yufit, M.R. Al–Haddad, J.C. Collings, F. Hartl, J.A.K. Howard, T.B. Marder, P.J. Low, *Inorg. Chim. Acta* **361** (2008) 1646–1658.
- [28] A.M. Sheloumov, A.A. Koridze, F.M. Doigushin, Z.A. Starikova, M.G. Ezernitskaya, P.V. Petrovskii, *Russ. Chem. Bull. Int. Ed.* **49** (2000) 1292–1296.
- [29] P. Braunstein, G. Predieri, A. Tiripichio, E. Sappa, *Inorg. Chim. Acta* **63** (1982) 113–118.
- [30] A.J. Deeming, S. Donovan–Mtunzi, K. Hardcastle, *J. Chem. Soc. Dalton Trans.* (1986) 543–545.
- [31] T. Adatia, M. McPartlin, *J. Chem. Soc. Dalton Trans.* (1988) 2889–2891.
- [32] M.I. Bruce, O.M. Shawkataly, B.K. Nicholson, *J. Organomet. Chem.* **286** (1985) 427–437.
- [33] M.J. Mays, P.R. Raithby, P.L. Taylor, K. Henrick, *J. Chem. Soc. Dalton Trans.* (1984) 959–967.
- [34] E. Delgado, B. Donnadiou, M.E. García, S. García, M.A. Ruiz, F. Zamora, *Organometallics* **21** (2002) 780–782.
- [35] H. Yao, R.D. McCargar, R.D. Allendoerfer, J.B. Keister, *Organometallics* **12** (1993) 4283–4285.
- [36] H. Yao, R.D. McCargar, R.D. Allendoerfer, J.B. Keister, A.A. Low, *J. Organomet. Chem.* **568** (1998) 63–76.
- [37] M.I. Bruce, E. Horn, O.B. Shawkataly, M.R. Snow, *J. Organomet. Chem.* **280** (1985) 289–298.
- [38] M.I. Bruce, N.N. Zaitseva, B.W. Skelton, A.H. White, *J. Organomet. Chem.* **690** (2005) 3268–3277.
- [39] M.I. Bruce, P.A. Humphrey, E. Horn, E.R.T. Tiekink, B.W. Skelton, A.H. White, *J. Organomet. Chem.* **429** (1992) 207–227.
- [40] H.M. Bell, NMR Simulator. Chemistry Department, Virginia Tech., Blacksburg, VA, 2004.
- [41] S. Kersch, A. Sebald, B. Wrackmeyer, *Magn. Reson. Chem.* **23** (1985) 514.
- [42] R.T. Morrison, R.N. Boyd, *Organic Chemistry*, sixth ed. Prentice–Hall Inc, New Jersey, 1992, p. 78, 273, 425.
- [43] Nonius, COLLECT. Nonius BV, Delft, The Netherlands, 2001.
- [44] Z. Otwinowski, W. Minor, *Methods in Enzymology*. Academic Press, New York, 1997, 307.
- [45] G.M. Sheldrick, *Acta Crystallogr.* **A64** (2008) 112–122.
- [46] L.J. Farrugia, *J. Appl. Cryst* **32** (1999) 837–838.